Developmental Cell, Vol. 9, 639–650, November, 2005, Copyright ©2005 by Elsevier Inc. DOI 10.1016/j.devcel.2005.09.011

Canonical Wnt Signaling and Its Antagonist Regulate Anterior-Posterior Axis Polarization by Guiding Cell Migration in Mouse Visceral Endoderm

Chiharu Kimura-Yoshida,[1,5] Hiroshi Nakano,[1,5] Daiji Okamura,[6] Kazuki Nakao,[3] Shigenobu Yonemura,[4] Jose A. Belo,[7,8] Shinichi Aizawa,[2,3] Yasuhisa Matsui,[6] and Isao Matsuo[1,5,*]

[1]Head Organizer Project, Vertebrate Body Plan Group
[2]Vertebrate Body Plan Group
[3]Laboratory for Animal Resources and Genetics Engineering Team
[4]Laboratory for Cellular Morphogenesis
RIKEN Center for Developmental Biology (CDB)
2-2-3 Minatojima-minami-cho
Chuou-ku Kobe
Hyogo 650-0047
Japan
[5]Department of Molecular Embryology
Osaka Medical Center and Research Institute for Maternal and Child Health
840 Murodo-cho
Izumi
Osaka 594-1101
Japan
[6]Cell Resource Center for Biomedical Research
Institute of Development, Aging, and Cancer
Tohoku University
Seiryo-machi 4-1
Sendai
Miyagi 980-8575
Japan
[7]Instituto Gulbenkian de Ciencia
Rua da Quinta Grande
6. Apartado 14
2781-901 Oeiras
Portugal
[8]Centro de Biomedicina Molecular e Estrutural
Universidade do Algarve
Campus de Gambelas
8005-139 Faro
Portugal

Summary

The mouse embryonic axis is initially formed with a proximal-distal orientation followed by subsequent conversion to a prospective anterior-posterior (A-P) polarity with directional migration of visceral endoderm cells. Importantly, *Otx2*, a homeobox gene, is essential to this developmental process. However, the genetic regulatory mechanism governing axis conversion is poorly understood. Here, defective axis conversion due to *Otx2* deficiency can be rescued by expression of *Dkk1*, a Wnt antagonist, or following removal of one copy of the *β-catenin* gene. Misexpression of a canonical Wnt ligand can also inhibit correct A-P axis rotation. Moreover, asymmetrical distribution of β-catenin localization is impaired in the *Otx2*-deficient and Wnt-misexpressing visceral endoderm. Concurrently, canonical Wnt and Dkk1 function as repulsive and attractive guidance cues, respectively, in the migration of visceral endoderm cells. We propose that Wnt/β-catenin signaling mediates A-P axis polarization by guiding cell migration toward the prospective anterior in the pregastrula mouse embryo.

*Correspondence: imatsuo@mch.pref.osaka.jp

Introduction

By embryonic day 5.5 (E5.5), the mouse embryonic axis is initially generated in a proximal-distal (P-D) orientation; subsequently, prior to gastrulation, this axis is converted to the anterior-posterior (A-P) direction (Beddington and Robertson, 1999). During the "axis rotation" process, a distinct population of visceral endoderm cells marked by *Hex* expression is located at the distal tip of the egg cylinder; these cells migrate proximally to the prospective anterior side of the embryo (Srinivas et al., 2004; Thomas et al., 1998). Coincidentally, in the proximal ectoderm region, several genes, *Cripto*, *Nodal*, and *Wnt(s)*, are expressed; furthermore, expression shifts to the posterior side, where the prospective primitive streak forms (Kimura et al., 2000, 2001; Thomas et al., 1998). Axis conversion involves the coordination of both anterior migration of distal visceral endoderm (DVE) cells and the posterior shift of proximal markers, which transforms the P-D orientation to the definitive A-P polarity.

A-P axis formation has been shown to be regulated by the TGF-β/Nodal signaling pathway. Notably, TGF-β/Nodal signaling promotes DVE formation; *Nodal* in the epiblast induces *Nodal* in the visceral endoderm as well as other target genes such as *Otx2* and *Nodal* antagonists, e.g., *Cerl* and *Lefty1* (Brennan et al., 2001). Additionally, the *Nodal* antagonists *Cerl* and *Lefty1* also participate in the formation of anterior visceral endoderm (AVE) by controlling cell proliferation in the visceral endoderm layer (Yamamoto et al., 2004).

Moreover, the axis conversion process requires the function of *Otx2*, a *paired*-type homeobox gene. The null mutation of the *Otx2* gene demonstrated axis rotation failure, resulting in a headless phenotype in the mouse embryo (Kimura et al., 2000; Perea-Gomez et al., 2001). Although *Nodal* antagonists *Cerl* and *Lefty1* were present in DVE of *Otx2*$^{-/-}$ embryos (Kimura et al., 2000; Perea-Gomez et al., 2001), *dickkopf1* (*Dkk1*), a Wnt antagonist, was absent (Kimura et al., 2001; Perea-Gomez et al., 2001; Zakin et al., 2000). These findings suggest that Wnt or other signaling pathways may be involved in axis rotation, in addition to *Nodal* signaling. However, the genetic mechanism by which *Otx2* controls A-P axis specification in terms of Wnt signaling remains unknown.

During axis specification in *Xenopus* embryos, canonical Wnt signaling is mediated by β-catenin (Logan and Nusse, 2004). In the absence of the Wnt ligand, β-catenin is constituitively phosphorylated by the serine threonine kinase, *GSK3*; subsequently, phosphory-

lated β-catenin is thought to undergo degradation. Upon inhibition of *GSK3* activity by Wnt signaling, dephosphorylated β-catenin translocates into the nucleus as an active form, and, consequently, β-catenin activates expression of specific target genes. A secreted Wnt antagonist, *Dkk1*, can bind Wnt coreceptors *LRP5/6* and degrade β-catenin indirectly (Glinka et al., 1998; Mao et al., 2002).

The current investigation provided evidence corresponding to a link between *Otx2* and Wnt/β-catenin signaling with respect to A-P axis polarization. Data suggested that *Dkk1*, which is a downstream target of *Otx2*, functions as an attractive guidance cue controlling directional migration of visceral endoderm cells and can inhibit the nuclear localization of β-catenin in visceral endoderm. Moreover, this study also demonstrated that defective DVE migration consequent to *Otx2* deficiency can be rescued by expression of *Dkk1* alone or heterozygosity of the *β-catenin* mutation. In conclusion, we propose that *Otx2* attenuates β-catenin activity in the visceral endoderm via Wnt antagonists including *Dkk1*, and that this serves as a mechanism to control Dkk1/Wnt-mediated guidance of DVE cell migration toward the future anterior side during A-P axis polarization.

Results

Expression of the *Dkk1* Gene during DVE Migration

We previously demonstrated that *Otx2*$^{-/-}$ embryos fail to form the A-P axis correctly (Kimura et al., 2000). Precise expression analysis of molecular markers during DVE migration involving whole-mount in situ hybridization revealed apparent normal formation of DVE in *Otx2*$^{-/-}$ embryos at E5.5, although migration to one side proximally was not possible (Figures 1A, 1B, 1A′, and 1B′). Expression of the DVE markers *Hex*, *Cerl*, and *Lefty1* was detected in the distal portion of visceral endoderm at E5.5 in *Otx2*$^{-/-}$ embryos, and this expression was similar to that of wild-type (Figures 1A, 1B, 1A′, and 1B′ and data not shown). Moreover, *Nodal* expression was normal in the epiblast of mutant embryos (Figures 1C and 1C′). At E6.5, expression of these markers remained in the distal portion of visceral endoderm and the proximal epiblast (Kimura et al., 2001, 2000; Perea-Gomez et al., 2001). These data clearly demonstrated that *Otx2*$^{-/-}$ embryos can form DVE normally around E5.5, whereas mutant DVE fails to migrate anteriorly even at E6.5.

In order to elucidate the role of *Dkk1* during DVE migration, *Dkk1* expression was examined in detail (Figures 1E–1K). Around E5.5, prior to migration, *Dkk1* expression was initially detected in the proximal portion of DVE in a circular pattern (Figures 1D–1F and 1H–1K). Importantly, *Dkk1* expression was negative in the most distal tip of the visceral endoderm, which is evidenced by the thickened morphology (Kimura et al., 2000); in contrast, *Hex* and *Cerl* expression was positive throughout the entire DVE (Figures 1A and 1B). *Dkk1* expression in *Otx2*$^{-/-}$ mutants at E5.5 was assessed to determine whether *Otx2* is necessary for induction of *Dkk1* expression from the initial phase or simply for maintenance at subsequent stages. Consequently, *Dkk1* expression was not observed in mutant embryos, which

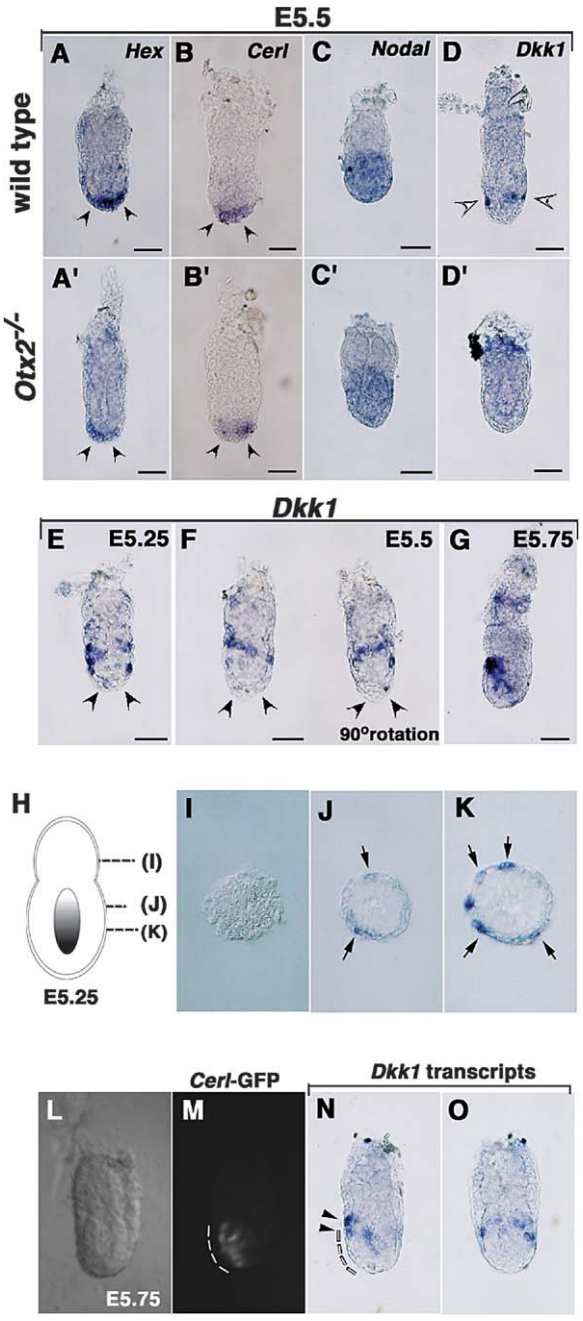

Figure 1. Marker Analysis of Wild-Type and *Otx2* Mutant Embryos during A-P Axis Development

(A–D′) Whole-mount in situ hybridization in (A–D) wild-type and (A′–D′) *Otx2*$^{-/-}$ embryos at E5.5. (A and A′) *Hex*, (B and B′) *Cerl*, (C and C′) *Nodal*, and (D and D′) *Dkk1*.

(E–G) *Dkk1* expression at (E) E5.25, (F) E5.5, and (G) E5.75.

(H–K) *Dkk1* expression at E5.25 in cross-sections at the level indicated in (H). Arrows indicate *Dkk1* expression.

(L–O) Comparative expression analysis of *Cerl* and *Dkk1* at E5.75. The GFP signal of the *Cerl-GFP* transgenic embryo was recorded, and, subsequently, *Dkk1* mRNA expression was examined by in situ hybridization. (L) Bright and (M) dark field views of the *Cerl-GFP* embryo. (N) Lateral and (O) frontal views of *Dkk1* expression of the *Cerl-GFP* embryo. (M and N) Dotted lines indicate the *Cerl*-positive domain. (N) Arrowheads indicate the *Dkk1*-positive domain.

Scale bars indicate 50 μm.

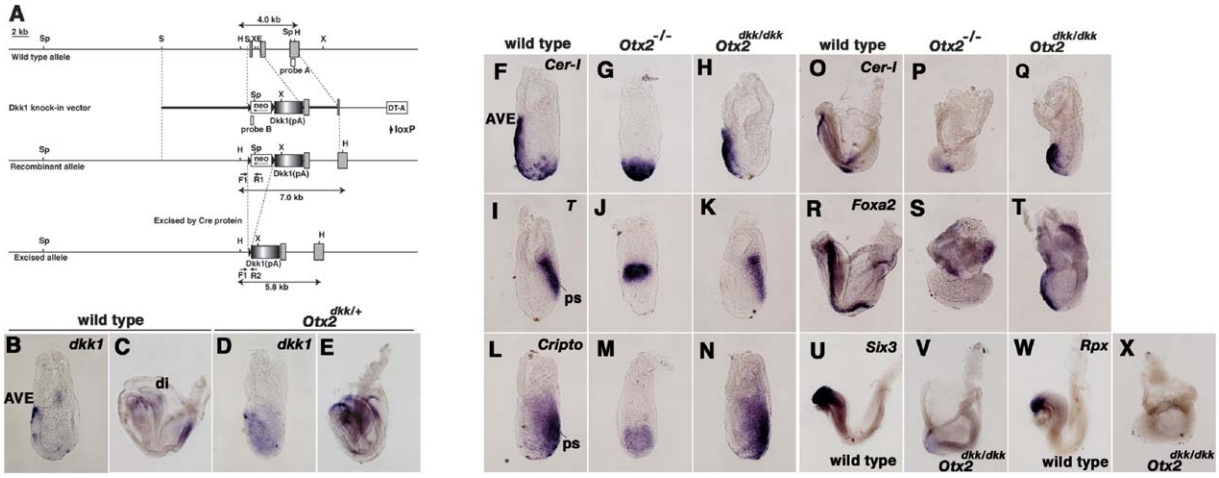

Figure 2. *Dkk1* Expression Rescues Axis Rotation Defects Caused by *Otx2* Mutation

(A) Generation of the *Dkk1* knockin mutation in the *Otx2* locus. Diagrammatic representations of the wild-type *Otx2* allele, knockin vector, recombinant allele, and excised allele. Probes A and B are those employed for Southern blotting to identify the knockin mutation.

(B–E) Whole-mount in situ hybridization with the *Dkk1* probe in (B and C) wild-type and (D and E) $Otx2^{dkk/+}$ embryos. (B and D) E6.5 and (C and E) E7.8.

(F–X) Whole-mount in situ hybridization in (F, I, L, O, R, U, and W) wild-type, (G, J, M, P, and S) $Otx2^{-/-}$, and (H, K, N, Q, T, V, and X) $Otx2^{dkk/dkk}$ embryos. (F–H and O–Q) *Cerl*, (I–K) *T*, (L–N) *Cripto*, (R–T) *Foxa2*, (U and V) *Six3*, and (W and X) *Rpx*. (F–N) E6.5, (O–T) E7.8, and (U–X) E8.0.

AVE, anterior visceral endoderm; di, diencephalic region; ps, primitive streak.

indicated that *Otx2* is essential for induction of *Dkk1* expression (Figure 1D′).

When DVE cells began to migrate to the anterior side by E5.75, *Dkk1* expression was observed in the future anterior side of the visceral endoderm; however, *Dkk1* expression was not evident in the posterior side (Figure 1G). Additional comparative expression analysis with *Cerl* and *Dkk1* revealed that *Dkk1*-positive visceral endoderm cells are apparently located in the foremost aspect of *Cerl*-positive migrating cells (Figures 1L–1O). These data suggest the possibility that asymmetrical *Dkk1* expression in the visceral endoderm might play a role in directional migration of DVE cells.

Dkk1 Expression Rescues Defective Axis Conversion Caused by *Otx2* Deficiency

In order to determine whether *Dkk1* participates in axis rotation as a downstream target of *Otx2*, mutant mice were generated in which the *Dkk1* cDNA was inserted into the *Otx2* locus ($Otx2^{dkk/+}$) (Figure 2). In the targeting vector, the *Otx2* gene was disrupted via insertion of *Dkk1* cDNA and the *PGKneo* cassette flanked by two *loxP* sites (Figure 2A; Figure S1; see the Supplemental Data available with this article online). Chimeras ($Otx2^{dkk\text{-}neo/+}$) were mated with *β-actin cre* transgenic mice in order to remove the *PGKneo* cassette. Normally, *Dkk1* is expressed in AVE at the gastrulation stage and in the presumptive diencephalic region at the subsequent head fold stage (Figures 2B and 2C) (Glinka et al., 1998). However, in $Otx2^{dkk/+}$ embryos, in addition to endogenous *Dkk1* expression domains, *Dkk1* expression was detected in the epiblast at E6.5 and in the entire rostral brain region at E7.8 (Figures 2D and 2E). Further RT-PCR analysis confirmed the absence of *Otx2* mRNA in $Otx2^{dkk/dkk}$ embryos (Figure S1). These findings clearly indicated that the knockin *Dkk1* cDNA is expressed correctly in lieu of the *Otx2* gene.

To determine whether axis rotation defects caused by the *Otx2* mutation can be restored upon replacement of *Dkk1* cDNA, several molecular markers were analyzed in $Otx2^{dkk/dkk}$ embryos (Figures 2F–2X). In $Otx2^{-/-}$ embryos, expression of the AVE markers *Cerl*, *Hex*, and *Lefty1* occur in the distal tip even at E6.5 (Figures 1A′, 1B′, and 2G; data not shown). Coincidentally, *T* expression is present in the proximal side, and *Cripto* expression is apparent in the entire epiblast of $Otx2^{-/-}$ embryos (Figures 2J and 2M). Importantly, in $Otx2^{dkk/dkk}$ embryos, expression of AVE markers *Cerl* and *Hex* was detected in AVE in a manner similar to that of wild-type embryos (Figure 2H; data not shown). Concurrently, *T* and *Cripto* expression were restricted normally to the posterior side of $Otx2^{dkk/dkk}$ embryos (Figures 2K and 2N). Restoration of axis conversion was observed frequently in $Otx2^{dkk/dkk}$ embryos (n = 20/50). These findings demonstrate that axis rotation defects due to the *Otx2* mutation can be partially rescued by *Dkk1* expression alone. In addition, *Otx2* regulates *Dkk1* expression in the AVE directly through Otx2 binding sites in the *Dkk1* promoter (Figures S2 and S3). As a result, the aforementioned data suggest that *Dkk1* can mediate axis conversion from the P-D to the A-P orientation as a crucial downstream target of *Otx2*.

The anterior neuroectoderm markers *Rpx*/*Hesx1* and *Six3* were examined to determine whether later forebrain abnormalities of $Otx2^{-/-}$ mutant embryos could be rescued by *Dkk1* cDNA (Figures 2U–2X). However, neither marker was induced in $Otx2^{dkk/dkk}$ embryos at E8.0 (Figures 2V and 2X; *Rpx*/*Hesx1*, n = 0/5; *Six3*, n =

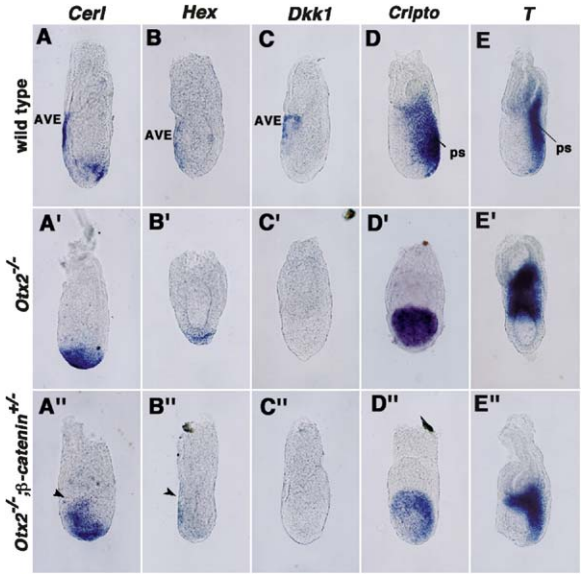

Figure 3. Rescue of A-P Axis Patterning Defects in *Otx2*$^{-/-}$;*β-catenin*$^{+/-}$ Embryos

(A–E″) Whole-mount in situ hybridization analysis of (A, A′, and A″) *Cerl*, (B, B′, and B″) *Hex*, (C, C′, and C″) *Dkk1*, (D, D′, and D″) *Cripto*, and (E, E′, and E″) *T* expression at E6.5; (A–E) wild-type, (A′–E′) *Otx2*$^{-/-}$, and (A″–E″) *Otx2*$^{-/-}$;*β-catenin*$^{+/-}$. AVE, anterior visceral endoderm; ps, primitive streak.

0/17). In order to assess whether failure in forebrain induction of *Otx2*$^{dkk/dkk}$ embryos is a consequence of anterior mesendoderm defects, expression of the molecular markers *Cerl* and *Foxa2* were analyzed (Figures 2O–2T). As expected, expression of these markers was severely affected in *Otx2*$^{dkk/dkk}$ embryos (Figures 2Q and 2T). This finding indicates that *Otx2*$^{dkk/dkk}$ embryos are unable to form the anterior mesendoderm properly. These results in concert suggest that failure of AVE migration may be primarily attributable to the absence of the Wnt antagonist, *Dkk1*, in *Otx2*$^{-/-}$ embryos; moreover, additional signaling molecules may be necessary for subsequent forebrain induction as previously proposed (Stern, 2001).

Rescue of Axis Rotation Defects in *Otx2*$^{-/-}$ Embryos Lacking One Copy of

Dkk1 inhibits canonical Wnt signaling at the extracellular level via direct interaction with *LRP5/6* and *Kremen*, which ultimately downregulates β-catenin activity in the nucleus (Mao et al., 2002). In order to examine genetic interaction between *Otx2* and Wnt/β-catenin signaling, *Otx2*$^{+/-}$ mutants were mated with mice carrying the *β-catenin* null allele; subsequently, double-mutant phenotypes were examined (Brault et al., 2001) (Figure 3). *Otx2*$^{+/-}$;*β-catenin*$^{+/-}$ mutants were viable and fertile (data not shown); as a result, *Otx2*$^{-/-}$;*β-catenin*$^{+/-}$ mice were obtained by crossing *Otx2*$^{+/-}$;*β-catenin*$^{+/-}$ mutants with *Otx2*$^{+/-}$ mutants. Molecular marker analysis was performed at E6.5 to analyze axis development in *Otx2*$^{-/-}$;*β-catenin*$^{+/-}$ embryos. *Cerl*, an AVE marker, expression in the DVE of *Otx2*$^{-/-}$ embryos was restricted to one side of the *Otx2*$^{-/-}$;*β-catenin*$^{+/-}$ visceral endoderm (Figures 3A, 3A′, and 3A″; n = 3/10). Similarly, proper expression of another AVE marker, *Hex*, was observed in the anterior side of the visceral endoderm in *Otx2*$^{-/-}$;*β-catenin*$^{+/-}$ embryos (Figure 3B″; n = 2/6). These findings indicate that the anterior migration defect of DVE cells in *Otx2* null mutants is partially rescued after removal of one copy of the *β-catenin* gene.

To establish whether restoration of *Otx2* null mutant defects is a consequence of ectopic induction of *Dkk1* expression due to heterozygosity of *β-catenin*, *Dkk1* expression was examined in these mutant embryos. However, *Dkk1* expression was never induced in *Otx2*$^{-/-}$;*β-catenin*$^{+/-}$ embryos (n = 0/6; Figure 3C″). Moreover, expression of posterior markers *Cripto* and *T* appeared to be restricted to one side of *Otx2*$^{-/-}$;*β-catenin*$^{+/-}$ embryos (n = 2/7, 2/4; Figures 4D″ and 4E″, respectively). These results, in concert, demonstrate that defective axis rotation in *Otx2*$^{-/-}$ embryos could be partially rescued after removal of one copy of the *β-catenin* gene. The aforementioned genetic evidence clearly supports *Otx2* participation in specification of A-P polarity via attenuation of Wnt/β-catenin signaling.

Misexpression of *Wnt8*, a Canonical Wnt Ligand, Prevents Axis Conversion from the P-D to the A-P Orientation

The aforementioned findings suggest the possibility that the attenuation of Wnt/β-catenin signaling can initiate A-P axis conversion in the mouse embryo. In order to determine whether attenuation of canonical Wnt signaling is essential for correct A-P axis formation during normal development, a transgenic mouse misexpressing the canonical Wnt ligand, mouse *Wnt8A* gene (*mWnt8A*), was generated; subsequently, phenotypes of these animals were analyzed (Figure S4 and Figure 4). *mWnt8A* is a mouse cognate of *Xenopus* Wnt8 and chicken *Wnt8c*, both of which possess strong double axis-inducing activity in frog and mouse, respectively (Popperl et al., 1997; Logan and Nusse, 2004). The Cre/loxP system was employed in order to examine precise phenotypes of transgenic embryos reliably during A-P axis development (Figure S4). The *lacZ* gene flanked by two *loxP* sites was inserted between the *CAG* promoter and *mWnt8A* cDNA. To remove the blockade of the *lacZ* stop codon, chimeras were mated with *β-actin-cre* transgenic mice, which ubiquitously express Cre protein (Lewandoski et al., 1997). *mWnt8A* expression was evaluated in the resultant *Tg(CAG-mWnt8A)* embryos to identify *mWnt8A* misexpression. Normally, *mWnt8A* expression occurs in the proximal epiblast prior to E6.0; subsequently, by E6.5, it is restricted to the posterior side (Figure S4 and Figure 4A). In contrast, hemizygous *Tg(CAG-mWnt8A)* embryos exhibited ectopic expression of the *mWnt8A* gene throughout the epiblast (Figure 4A′).

Morphological analysis of *Tg(CAG-mWnt8A)* embryos revealed failure to specify the embryonic region of the visceral endoderm appropriately at E6.5 (Figures 4B–4E and 4B′–4E′). Wild-type embryos lost their symmetrically cylindrical shape; additionally, distinct curvatures were apparent on the opposite side of the primitive steak at this stage (Figure 4B). In contrast, the

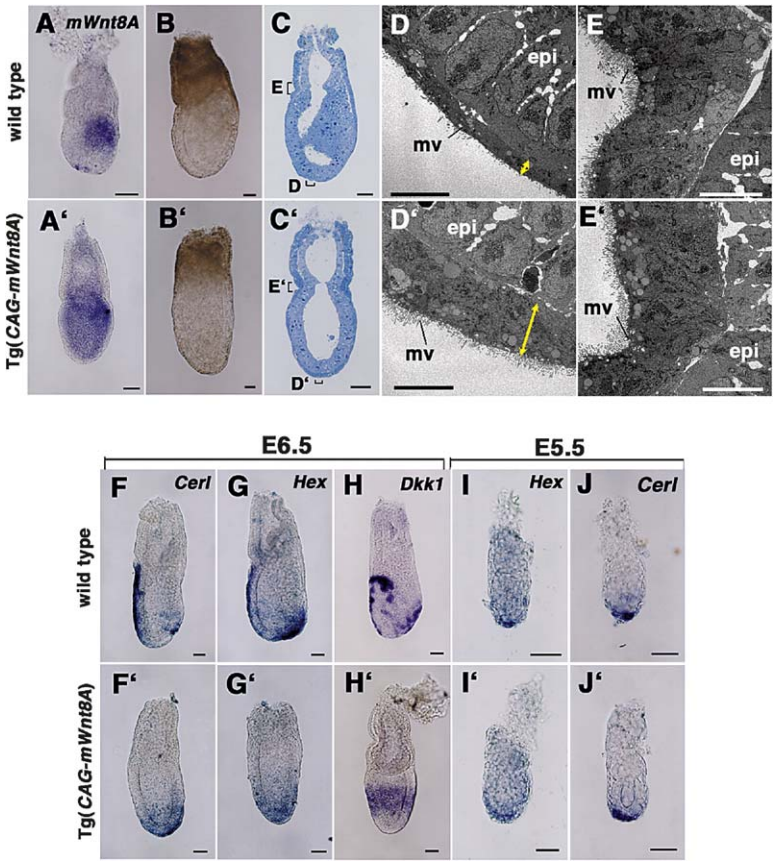

Figure 4. Morphological and Molecular Marker Analyses of *Tg(CAG-mWnt8A)* Embryos

(A–J′) Whole-mount in situ hybridization in (A and F–J) wild-type and (A′ and F′–J′) *Tg(CAG-mWnt8A)* embryos; (A and A′) *mWnt8A*, (F, F′, J, and J′) *Cerl*, (G, G′, I, and I′) *Hex*, and (H and H′) *Dkk1* at (I, I′, J, and J′) E5.5 and (A, A′, F–H, F′–H′) E6.5. Morphological analysis of (B–E) wild-type and (B′–E′) transgenic embryos at E6.5. Fine structure of embryos by (C and C′) semithin sections and corresponding (D, D′, D, and E′) electron micrographs. Scale bars are 50 μm in (A)–(C), (A′)–(C′), (F)–(J), and (F′)–(J′) and are 10 μm in (D), (D′), (E), and (E′). epi, epiblast; mv, microvilli.

external morphology of *Tg(CAG-mWnt8A)* embryos was nearly symmetrical, and curvature was not evident at E6.5 (Figure 4B′). The size of *Tg(CAG-mWnt8A)* embryos was nearly identical to that of wild-type embryos; consequently, morphological abnormalities are not attributable to developmental retardation.

Subsequently, fine structure was examined via utility of semithin and ultrathin sections to assess the visceral endoderm structure more precisely. These experiments revealed that embryonic visceral endoderm is improperly regionalized in these embryos (Figures 4C–4E and 4C′–4E′). In wild-type embryos, visceral endoderm cells of the extraembryonic region displayed a tall, columnar appearance and a high degree of vacuolization in association with dense microvilli, whereas the embryonic region consisted of squamous cells with lower numbers of microvilli (Figures 4D and 4E) (Batten and Haar, 1979). DVE cells of *Tg(CAG-mWnt8A)* embryos possessed a tall, columnar shape, but not a squamous shape, and many microvilli, characteristics identical to those of visceral endoderm cells at the level of the extraembryonic region (Figures 4D′ and 4E′). However, morphological features of epiblast cells were unchanged in the *Tg(CAG-mWnt8A)* embryos (Figures 4D and 4D′). These findings suggest that misexpression of *mWnt8A* leads to developmental failure of visceral endoderm, but not of epiblasts.

To further assess A-P axis phenotypes in transgenic embryos, several marker genes were examined at the gastrulation stage (Figures 4F–4J and 4F′–4J′). Expression of AVE markers *Cerl*, *Hex*, and *Lhx1* was observed in the DVE of *Tg(CAG-mWnt8A)* embryos; expression was not shifted to one side at E6.5 (Figures 4F′ and 4G′; data not shown). Circular, symmetrical *Dkk1* expression remained in the proximal portion of DVE; however, it was not restricted to the anterior side (Figure 4H′). Notably, expression of *Cerl* and *Hex* occurred normally in DVE of the transgenic embryos at E5.5, suggesting that DVE is formed appropriately in *Tg(CAG-mWnt8A)* embryos (Figures 4I′ and 4J′). Concurrent with these findings, in terms of posterior markers, proximal *T* expression remained, and *Cripto* and *Nodal* expressions were apparent throughout the entire epiblast of *Tg(CAG-mWnt8A)* embryos at E6.5 (Figure S5). The aforementioned data demonstrate that misexpression of *mWnt8A* leads to failure of axis conversion with respect to the P-D to the A-P orientation.

Asymmetrical Distribution of β-Catenin Localization in the Visceral Endoderm Is Impaired in *Otx2*-Deficient and *Tg(CAG-mWnt8A)* Embryos

These lines of evidence suggest the possibility that, during normal A-P axis development, β-catenin activity is attenuated in AVE. In order to test this point directly, expression and cellular localization of the active form of β-catenin, which is dephosphorylated at residues Ser37 and Thr41 (Staal et al., 2002), was analyzed via confocal immunofluorescence. Findings indicate that nuclear and cytoplasmic β-catenin is specifically diminished in AVE of wild-type embryos (Figures 5A and 5B).

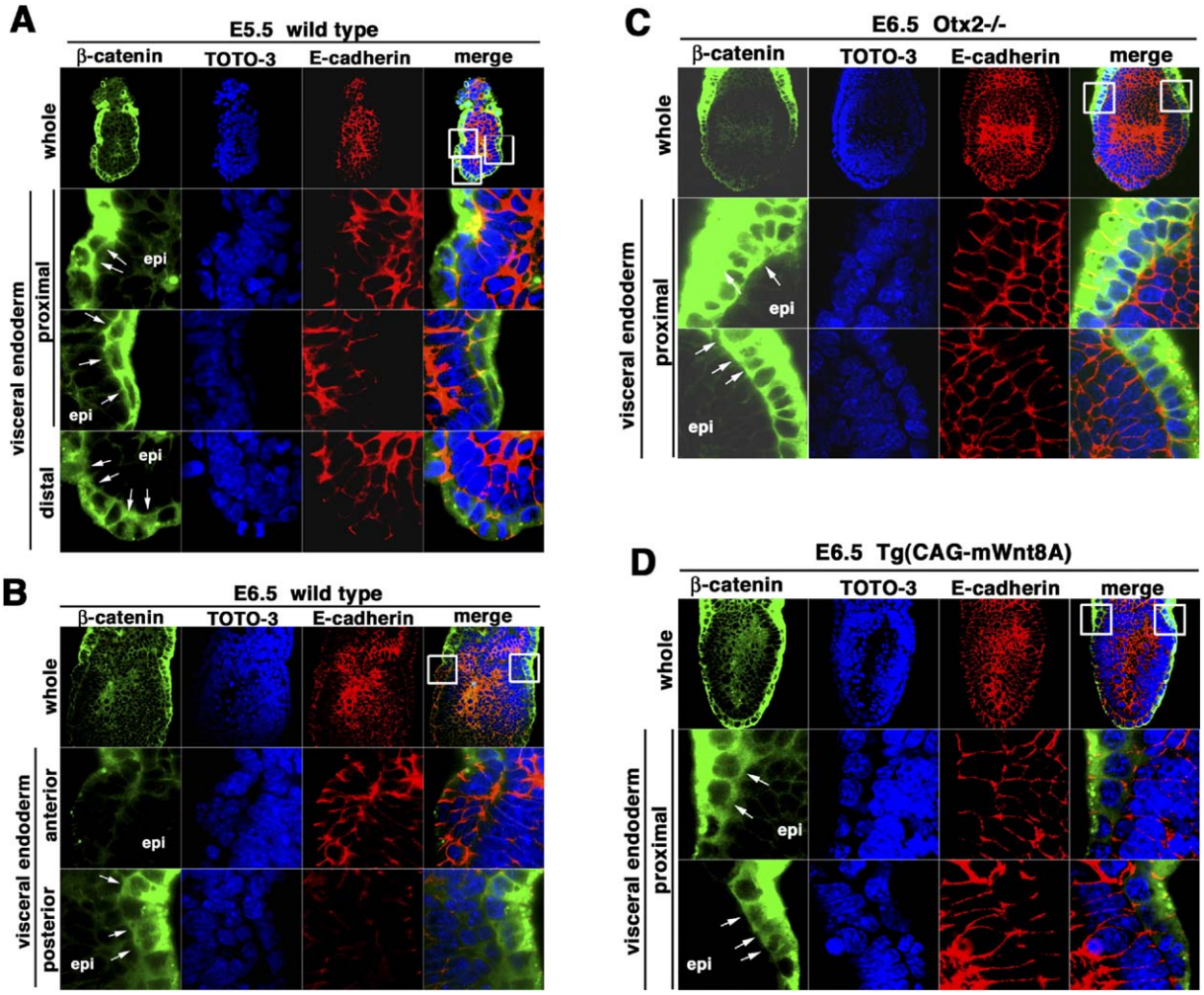

Figure 5. Expression and Cellular Localization of the Active Form of the β-Catenin Protein during A-P Axis Specification

(A–D) Fluorescent images of (A and B) wild-type, (C) *Otx2*$^{-/-}$, and (D) *Tg(CAG-mWnt8A)* embryos at (A) E5.5 and (B–D) E6.5. (A–D) Anti-active-β-catenin (green), TOTO-3 (nuclei, blue), E-cadherin (adherens junctions, red), and the merged image. The areas shown in the magnified views are marked in the upper merged images (white squares). (A) Active-β-catenin protein is strongly detected in the cytoplasm of the entire visceral endoderm as well as in the nucleus, where the TOTO-3 image is merged (white arrows). (B) Nuclear and cytoplasmic β-catenin expression is upregulated in the posterior visceral endoderm (white arrows). (C) Localization of nuclear β-catenin is evident in both proximal aspects of the visceral endoderm (white arrows). (D) Nuclear β-catenin localization is observed in the proximal visceral endoderm (white arrows). epi, epiblast.

At E5.5, β-catenin is substantially localized in the cytoplasm of the entire visceral endoderm at the level of both embryonic and extraembryonic regions (Figure 5A). Additionally, β-catenin was frequently localized in the nucleus of the proximal and distal aspects of the embryonic visceral endoderm region. However, in the epiblast, β-catenin is uniformly present at the cell surface, although it is never observed in the cytoplasm and nucleus. These findings afford evidence that β-catenin is uniformly distributed in the embryonic visceral endoderm region at E5.5; moreover, Wnt/β-catenin signaling may be activated more strongly in the visceral endoderm than in the epiblast.

At E6.5, cytoplasmic and nuclear β-catenin were distributed in the visceral endoderm layer, but not in the epiblast, a situation similar to that at E5.5 (Figure 5B). However, cytoplasmic and nuclear β-catenin was markedly diminished in AVE; in contrast, it was elevated in posterior visceral endoderm (Figure 5B). This asymmetrical distribution of β-catenin in conjunction with the A-P axis could be observed initially around E5.75, when DVE cells migrate to the anterior side (data not shown). These data demonstrate that nuclear and cytoplasmic β-catenin are asymmetrically distributed in the visceral endoderm layer along with the A-P axis in the mouse embryo.

In order to address whether asymmetrical distribution of β-catenin is impaired in *Otx2*$^{-/-}$ mutant embryos, expression and cellular localization of β-catenin were analyzed at E6.5 (Figure 5C). Cytoplasmic and nuclear β-catenin, which are elevated throughout the entire embryonic visceral endoderm region, did not exhibit obvious asymmetrical distribution in *Otx2*$^{-/-}$ embryos. However, in mutant epiblasts, β-catenin was uniformly

localized exclusively at the cell surface in a manner similar to that in wild-type embryos. These findings provide direct evidence that asymmetrical distribution of cytoplasmic and nuclear β-catenin cannot occur in the *Otx2*$^{-/-}$ visceral endoderm layer; moreover, these data indicate that *Otx2* is required to reduce cytoplasmic and nuclear β-catenin expression in AVE.

To ascertain whether the reduction of cytoplasmic and nuclear β-catenin expression in AVE is necessary for correct A-P axis development, β-catenin expression was examined in *Tg(CAG-mWnt8A)* embryos, which exhibit migratory defects of DVE cells as described (Figure 4). Consequently, reduction of cytoplasmic and nuclear β-catenin expression in visceral endoderm did not occur in the transgenic embryos (Figure 5D). In *Tg(CAG-mWnt8A)* embryos, β-catenin expression was strongly upregulated in the cytoplasm as well as in the nucleus of the visceral endoderm layer. Unexpectedly in the epiblast, β-catenin expression was unchanged; it was detected exclusively at the cell surface in a manner identical to that of the wild-type. Therefore, these findings suggest that reduction of β-catenin expression in AVE may be crucial for correct A-P axis rotation; moreover, failure of AVE migration observed in *Tg(CAG-mWnt8A)* embryos may be due primarily to the visceral endoderm, but not to the epiblast.

Dkk1 and Wnt Can Function as Attractive and Repulsive Guidance Cues, Respectively, Controlling Directional Migration of Visceral Endoderm Cells

The aforementioned findings lend support to the regulation of visceral endoderm cell migration by Wnt/β-catenin signaling. One possible mechanism by which Wnt/β-catenin signaling controls cell migration involves attractive mediation by *Dkk1* and/or repulsive mediation by *Wnt*, which function as guidance cues. In order to address this issue, migratory behavior of DVE cells was analyzed with recombinant protein-soaked beads in whole-embryo culture. Results reveal that Dkk1 attracts and that Wnt3A repels migratory DVE cells (Figure 6).

To identify migratory DVE cells, *Cerl-GFP* transgenic embryos were employed; this strain permits labeling of migrating visceral endoderm cells from E5.5 to E6.5 via the fluorescent microscopy (Belo et al., 1997; Mesnard et al., 2004). E5.5–E5.75 transgenic embryos were embedded in a gel-matrix medium for three-dimensional culture (see Experimental Procedures); beads coated with a recombinant protein were located at the proximal side of the embryos (Figure 6A). During the whole-embryo culture for 5–48 hr, GFP-positive cell behavior was analyzed under the fluorescent microscope; subsequently, behavior was classified into four types (Figures 6A and 6B, Types I–IV). In the case in which a BSA-soaked bead was embedded in the proximal side of the embryo prior to migration of GFP-positive cells, DVE cells migrated randomly irrespective of the position of BSA beads (Figure 6B) (the same side of the bead, Type I, n = 4/10; the opposite side of the bead, Type II, n = 4/10). Notably, when a Dkk1-soaked bead was embedded in the proximal side of the embryo prior to cell migration, DVE cells consistently migrated to the same side of the Dkk1 bead (Figures 6B and 6C) (Type I + III, n = 13/16); these cells migrated to the same side exclusively (Type I, n = 7/16), or they migrated in two distinct directions, the same and opposite sides (Type III, n = 6/16). This finding suggests that Type III migration occurs as a result of the attraction of DVE cells by two Dkk1 sources: endogenous Dkk1 expression at the opposite side and embedded Dkk1.

Next, a Dkk1-soaked bead was embedded in the prospective posterior side of the embryo after initiation of anterior migration of GFP-positive cells (Figure 6B). As a result, migrating visceral endoderm cells altered direction and migrated to the same side of the Dkk1 bead (Type I + III, n = 9/10); the entire population of these cells migrated to the same side, the prospective posterior side (Type I, n = 3/10), or they migrated in two distinct directions, the prospective anterior and posterior sides (Figures 6B and 6D; Type III, n = 6/10). In contrast, when a Dkk1 bead was embedded in the prospective anterior side after initiation of anterior migration of cells (Figure 6B), the Dkk1 bead did not alter the direction of approaching DVE cells (Type I, n = 9/9). These observations clearly demonstrate that Dkk1 protein can attract DVE cells prior to and during movement.

On the other hand, in the case in which a bead soaked with Wnt3A, a canonical Wnt ligand, was embedded in the proximal side prior to cell migration, GFP-positive cells did not migrate to the same side of the bead (Type I, n = 0/10); rather, these cells migrated to the opposite side (Type II, n = 5/10), or they failed to migrate (Type IV, n = 5/10; Figures 6B and 6E). When the 40 ng/μl Wnt3A-soaked bead was embedded in the prospective anterior side, the direction of migrating visceral endoderm cells was unaffected (Figure 6B) (Type I, n = 8/11). However, a bead soaked at a 10-fold lower concentration (4 ng/μl) efficiently repelled the migrating DVE cells (Type II + III + IV, n = 12/19). Additionally, when the Wnt3A bead was embedded in the prospective posterior side after initiation of anterior migration of cells (Figure 6B), the Wnt3A bead did not alter the direction of receding DVE cells (Type III, n = 6/7). These findings suggest that Wnt3A can repel DVE cells prior to and during movement.

In order to determine whether embedded protein-soaked beads mediate cell migration via alteration of activity of Wnt/β-catenin signaling, β-catenin expression in explants containing the beads was examined by confocal microscopy (Figure 6F). After a 5 hr incubation, the BSA bead failed to alter symmetrical β-catenin expression in the visceral endoderm layer (Figure 6F). However, after a 5 hr incubation with the Dkk bead, the visceral endoderm layer displayed asymmetrical β-catenin expression along the prospective A-P axis; the Dkk1 side exhibited dramatic reduction of β-catenin expression, whereas the opposite side demonstrated upregulation of β-catenin (Figure 6F). These findings strongly suggest that asymmetrical Wnt/β-catenin signaling in the prospective A-P axis of the pregastrula embryo provides the morphogenetic force that drives the directional displacement of the DVE cells.

Discussion

The present investigation demonstrates that *Otx2* specifies A-P polarity via attenuation of Wnt/β-catenin signaling in the prospective anterior side of the mouse

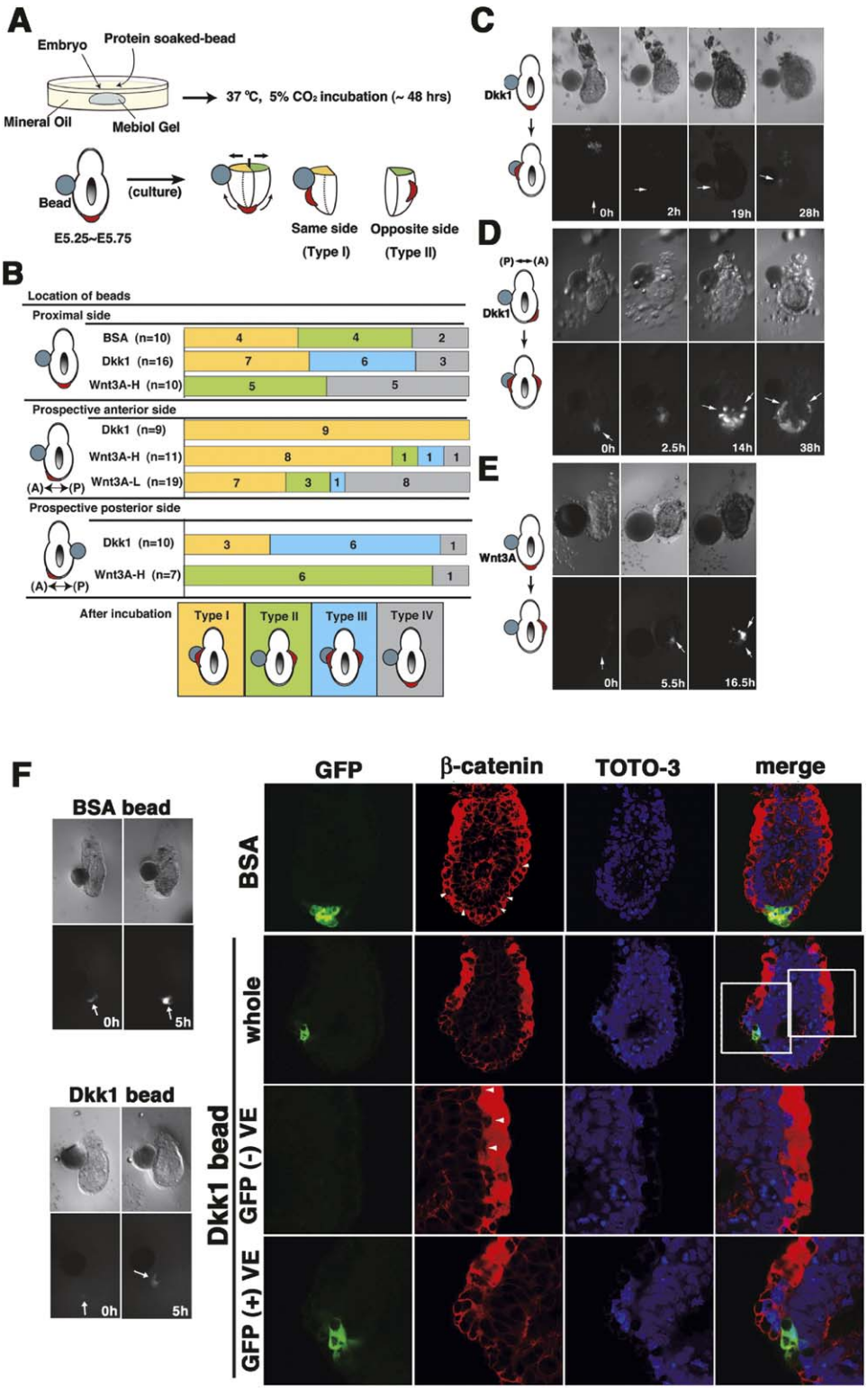

Figure 6. Dkk1 and Wnt3A Act as Guidance Cues Controlling the Migratory Direction of DVE Cells

(A and B) Experimental strategy and summary of bead explants. *Cerl-GFP* transgenic embryos were embedded in the medium gel with protein-soaked beads. After culture, the positions of GFP-positive DVE cells were classified into four types as illustrated (Types I–IV): Type I (orange), same side as the explanted bead; Type II (green), opposite side of the explanted bead; Type III (light blue), both the same and the opposite sides of the explanted bead; Type IV (gray), distal side of the embryo. Two different concentrations of Wnt3A beads were used: 40 ng/μl (Wnt3A–H) and 4 ng/μl (Wnt3A–L).

(C) Example of the Dkk1 protein-soaked bead embedded in the proximal side of the embryo (Type I).

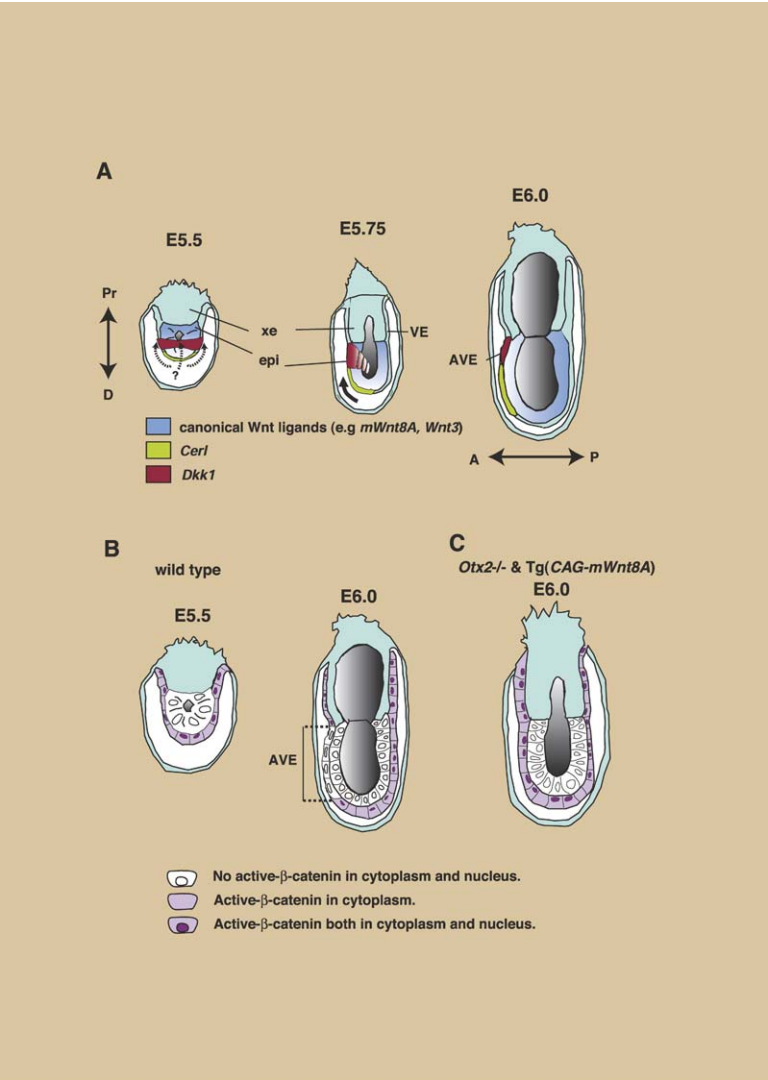

Figure 7. Schematic Model of the Mechanism Governing A-P Axis Development via Wnt/β-Catenin Signaling in the Mouse Embryo

(A) Schematic representation of wild-type mouse embryos between E5.5 and E6.0. At E5.5, DVE cells are thought to possess the ability to migrate in the proximal direction marked by the *Dkk1*-positive domain (dotted arrows). At E5.75, Wnt/β-catenin signaling is attenuated by anterior restriction of *Dkk1* expression. Direction of DVE cell migration is indicated by an arrow. By E6.0, *Dkk1* expression is detected in the most anterior portion of AVE; furthermore, axis conversion is completed in the A-P direction.

(B and C) Schematic diagrams regarding expression of active-β-catenin in the wild-type at E5.5 and E6.0 and in the *Otx2*$^{-/-}$ and *Tg(CAG-mWnt8A)* embryos at E6.0. (B) At E5.5, cytoplasmic and nuclear β-catenin is localized in the visceral endoderm layer, but not in the epiblast layer; at subsequent E6.0, cytoplasmic and nuclear β-catenin expression is reduced anteriorly and upregulated posteriorly in the wild-type. (C) In the migration-defective embryos, cytoplasmic and nuclear β-catenin expression is symmetrically distributed in the entire visceral endoderm even at E6.0. A, anterior; AVE, anterior visceral endoderm; D, distal; epi, epiblast; P, posterior; Pr, proximal; VE, visceral endoderm; xe, extraembryonic ectoderm.

embryo. The Wnt antagonist Dkk1, which is a crucial downstream target of *Otx2*, acts as an attractive guidance cue controlling the directional migration of visceral endoderm cells. Moreover, to our knowledge, this genetic evidence provides novel insights into evolutionarily conserved mechanisms governing primary body axis formation in metazoans.

Wnt/β-Catenin Signaling Regulates A-P Axis Development

Our findings led to the proposal of a model describing the role of Wnt/β-catenin signaling in A-P axis development of the mouse embryo (Figure 7). Normally, prior to AVE migration, around E5.5, a canonical Wnt antagonist, *Dkk1*, is expressed in the proximal portion of DVE cells in a circular, symmetrical pattern (Figures 7A). On the other hand, canonical Wnt ligands, e.g., *mWnt8A* and *Wnt3*, are expressed in the proximal epiblast (Figure 7A). At this stage, any proximal direction may be competent with respect to migration of DVE cells, as suggested by symmetrical *Dkk1* expression. However, β-catenin expression does not appear to be downregulated in these *Dkk1*-positive domains. This delayed attenuation of β-catenin expression is probably attributable to the time lag associated with protein degradation of β-catenin or to insufficient levels of *Dkk1* expression.

(D) Example of the Dkk1 protein-soaked bead embedded in the prospective posterior side of the embryo (Type III).

(E) Example of the Wnt3A-H protein-soaked bead embedded in the proximal side of the embryo (Type II). GFP-positive cells are indicated by white arrows in (C)–(E).

(F) The BSA or Dkk1 protein-soaked beads embedded in the proximal side of the embryo for β-catenin expression analysis. After a 5 hr incubation, *Cerl*-positive cells do not migrate to one side in the BSA-embedded explant, while these cells start to migrate to one side in the Dkk1-embedded explant. Cerl-GFP (green), anti-active-β-catenin (red), TOTO-3 (nuclei, blue), and the merged image. The areas shown in the magnified views are marked in the upper merged images (white squares).

By E5.75, attenuation of Wnt/β-catenin signaling in the AVE is closely linked with the axis conversion process from the P-D to the A-P orientation. Axis rotation may occur primarily as a result of asymmetrical expression of Wnt antagonists, including *Dkk1*. Concurrently, *Dkk1* expression is downregulated in the prospective posterior side and upregulated in the anterior side, whereas β-catenin expression displays the opposite profile (Figures 7A and 7B).

Wnt signaling has been classified into two pathways: the canonical and noncanonical pathways, or *β-catenin*-dependent and -independent pathways, respectively (Logan and Nusse, 2004). The current study demonstrates that the canonical Wnt antagonist, *Dkk1*, and its nuclear target, β-catenin, participate in DVE migration. Additionally, misexpression of a canonical Wnt ligand, *mWnt8A*, prevented correct A-P axis conversion (Figure 4). Coincidentally, asymmetrical distribution of β-catenin expression was not observed in the AVE of *Otx2*-deficient and *Tg(CAG-mWnt8)* embryos (Figures 5 and 7C). These results, in concert, strongly support the crucial role of asymmetrical β-catenin localization in A-P axis conversion. However, *Dkk1* homozygous mutant embryos appeared to undergo normal A-P axis development (Mukhopadhyay et al., 2001). To account for this disparity, other inhibitory molecules of Wnt/β-catenin signaling, which complement the *Dkk1* function in visceral endoderm at different levels of the signaling pathway, may be present, albeit at reduced levels in *Otx2*-deficient embryos, e.g., *Cerl*, *Axin*, *TCF3*, *Wise*, and *ICAT* (Logan and Nusse, 2004).

Wnt/β-Catenin Signaling Guides Directional Migration of Visceral Endoderm Cells

This investigation provides for the evidence that the canonical Wnt ligand and its antagonist function as guidance cues in the DVE cell migration. Migrating visceral endoderm cells possess unique morphology distinct from that of adjacent endoderm cells, as well as active migratory character; these cells continuously change shape and project filopodial processes (Kimura et al., 2000; Srinivas et al., 2004). Comparative expression analysis of *Dkk1* with *Cerl* suggests that *Dkk1*-positive cells are located at the forefront of migratory DVE cells (Figure 1). These findings suggest that *Dkk1* may determine the migratory direction of DVE cells. Moreover, apparent normal expression of *Nodal* and its antagonists in *Otx2*-deficient embryos (Figure 1) might afford evidence in support of the previously described observation that $Otx2^{-/-}$ DVE cells display no significant change with respect to cell proliferation; rather, they exhibit a defect associated with directional migration (Perea-Gomez et al., 2001). Further BrdU incorporation experiments with Wnt8A-misexpressing embryos and Dkk1/Wnt3A-embedded explants revealed that Wnt ligands and Dkk1 failed to mediate asymmetrical cell proliferation along with the A-P axis (C.K.-Y., D.O., Y.M., and I.M., unpublished data). In a manner consistent with these notions, Dkk1 can attract *Cerl*-positive DVE cells and a canonical Wnt ligand, Wnt3A, can repel them as a migratory guidance cue (Figure 6). Furthermore, attenuation of β-catenin expression in the cytoplasm and the nucleus during DVE cell migration appears to be linked to asymmetrical expression of *Dkk1* and the embedded Dkk1 bead (Figures 5 and 6). In conjunction, these findings directly support mediation of the directional migration of DVE cells by the combination of Wnt-mediated repulsion and its antagonist-mediated attraction.

Otx2 May Regulate Asymmetrical Distribution of *β-Catenin* Activity in Conjunction with the Primary Body Axis

This study indicates that localization of the dephosphorylated form of β-catenin is dynamically regulated during A-P axis specification (Figures 5, 7B, and 7C). In the wild-type visceral endoderm layer, cytoplasmic and nuclear β-catenin expression are specifically reduced in the prospective anterior side. Notably, in both *Otx2*-deficient and *Tg(CAG-mWnt8A)* embryos, which display failure of axis rotation, the expression is not downregulated; rather, it is upregulated throughout the entire visceral endoderm layer (Figures 5 and 7). Although further molecular analysis is necessary in order to elucidate the precise molecular mechanism by which *Dkk1* expression is initially induced in the most proximal portion of DVE and subsequently downregulated in the prospective posterior side, *Otx2* expression is crucial for *Dkk1* expression in the visceral endoderm (Figures S2 and S3). In addition, *Dkk1* alone can rescue axis rotation failure attributable to *Otx2* deficiency (Figure 2). These findings suggest that *Otx2* specifies A-P axis development primarily via regulation of Wnt/β-catenin signaling pathways, including *Dkk1*, in the visceral endoderm.

Surprisingly, *mWnt8A* transcripts driven by the *CAG* promoter are upregulated primarily in the epiblast, but not in the visceral endoderm (Figure 4A′), whereas expression of the dephosphorylated form of β-catenin is not elevated in the epiblast layer of *Tg(CAG-mWnt8A)* embryos. This finding suggests the involvement of unexpected molecular mechanisms via which Wnt signaling can be transmitted to β-catenin activity mainly in the visceral endoderm, but not in the epiblast layer.

To our knowledge, this genetic evidence affords novel insights into evolutionarily conserved mechanisms governing primary body axis formation across the metazoans. The asymmetrical distribution of β-catenin activity along with the A-P axis plays a pivotal role in the specification of A-P polarity throughout metazoan embryos. In amphibians, fish, ascidians, sea urchins, and cnidarians, β-catenin is localized to cell nuclei preferentially at one pole of the cleavage-stage embryo (Imai et al., 2000; Logan et al., 1999; Schneider et al., 1996; Wikramanayake et al., 2003). In these various organisms, nuclear activity of *β-catenin* is required for early axis specification and the subsequent establishment of critical signaling centers, "organizers", in the early embryo. The present investigation suggests that asymmetrical distribution of β-catenin expression serves as a primary mediator of axis specification in the mammalian embryo.

Experimental Procedures

Construction of Targeting Vector for *Dkk1* Knockin Mice

In the targeting construct, *Dkk1* cDNA with polyadenylation signals and the *PGKneo* cassette were inserted into the SmaI and the

EcoRI sites, located 220 bp upstream from the translation initiation site and in the first intron, respectively. Homologous recombinant TT2 ES cells and chimeric mice were obtained as described (Matsuo et al., 1995).

Generation of *CAG-mWnt8A* Transgenic Mice

Mouse *Wnt8A* cDNAs were isolated from a mouse cDNA library. In brief, *mWnt8A* cDNA fused with a *CAG* promoter (Niwa et al., 1991) was ligated to the *lacZ* gene flanked by two *loxP* sites. Subsequently, a *CAG-lacZ-mWnt8A* transgene was constructed via ligation of the aforementioned resultant vectors with the *neo* gene driven by the *PGK1* promoter with a polyadenylation signal. TT2 ES cells were cultured, electroporated with linearized transgenic vectors, and selected in G418 (Figure S4).

Genotyping

Transgenic and knockin founders and their progenitors were routinely determined by PCR. Primers and lengths of the products in the PCR analyses were as follows: in the transgenic mice, *CAG-lacZ-mWnt8A* was identified with primers *CAG-pro* (5′-TAGAGC CTCTGCTAACCATGTTCATGCCTT-3′) and *CAG-lacZ* (5′-AGTGTC CCAGCCTGTTTATCTACGGCTTAA-3′), yielding 270 bp. The *CAG-mWnt8* allele excised by Cre was determined with primers *CAG-pro* and *CAG-mWnt8A* (5′-GATGGCAGCAGAGCGGATGGCATGAAT GAA-3′), yielding 500 bp. *Dkk1* knockin mice were identified with the following primers: wild-type *Otx2* allele with primers *Forward1* (5′-GTATTTTCCTTGCTACCAAACTGCCGAGTG-3′) and *Reverse1* (5′-CTGGAGGGAAGCCACACCTCTAAGGATTAA-3′), yielding 400 bp, and *Dkk1* knockin allele with primers *Reverse1* and *SVDK-2* (5′-ACAGCAGAAACATACAAGCTGTCAGCTTTG-3′), yielding 200 bp. *β-catenin* mutant mice were obtained from the Jackson Laboratory and genotyped as described (Brault et al., 2001).

Expression Analysis and Semi- and Ultrathin Sections

In situ hybridization was performed as described (Wilkinson, 1998). For morphological analysis, embryos were fixed in 2% paraformaldehyde plus 2.5% glutaraldehyde in 0.1 M sodium cacodylate buffer (pH 7.3); subsequently, tissues were postfixed for 2 hr in 1% OsO4 and were embedded in Poly Bed 812. Semithin sections (0.55 μm thickness) were produced with a glass knife and stained with 0.5% toluidine blue. Ultrathin sections (70 nm thickness) were obtained with a diamond knife and examined after staining with uranyl acetate and lead citrate.

Whole-Embryo Culture with Recombinant Protein Beads

Female ICR mice were sacrificed between 10:00 and 17:00 hr on the fifth day of pregnancy. Embryos were dissected from decidual tissue in M2 medium lacking Phenol red. The GFP-positive embryos, which were collected under a fluorescent microscope (Leica), were cultured in the Mebiol Gel matrix (Mebiol, Inc.) containing 50% DMEM and 50% rat serum in 5% CO_2 at 37°C for 5–48 hr for three-dimensional culture. Images of migratory behavior of visceral endoderm cells were captured and recorded with a Hamamatsu chilled CCD camera (C5985). Beads (Affigel Bluo Gel, BioRad) were rinsed in PBS several times and soaked in 200 ng/μl mouse Dkk1 recombinant protein (R&D system), 40 and 4 ng/μl mouse Wnt3A recombinant protein (R&D System), or 50 mg/ml BSA-PBS solution overnight at 4°C or for 1 hr at 37°C. Prepared beads were transplanted to the proximal side of the embedded transgenic embryo.

Immunohistochemistry

Wild-type, *Otx2*$^{-/-}$, *Tg(CAG-mWnt8A)*, and *Cerl-GFP* embryos were fixed as described (Ciruna and Rossant, 2001). Primary antibodies were applied at the following concentrations: 10 mg/ml for rat anti-E-cadherin (ECCD-2) (Takara Shuzo) and at a 1:300 dilution for anti-active-β-catenin (anti-ABC) (8E7) (Upstate). Appropriate species-specific, fluorophore-labeled secondary antibodies (Molecular Probes) were applied at 1:200 dilution. Nuclei were stained with TOTO-3 iodide (Molecular Probes) at a 1:500 dilution in the presence of 100 μg/ml RNase A. Staining was examined with a confocal microscope (Leica).

Supplemental Data

Supplemental Data including five figures are available at http://www.developmentalcell.com/cgi/content/full/9/5/639/DC1/.

Acknowledgments

We are grateful to Drs. E. De Robertis, R. Grosschedl, B.G. Herrmann, B. Hogan, G. Martin, R. Nusse, M.M. Shen, and K. Yamamura for in situ probes. We also wish to thank Dr. C. Niehrs for *Dkk1* cDNA plasmid; the Animal Resources and Genetic Engineering Team, RIKEN Center for Developmental Biology for housing the mice; and Ms. Naoko Inoue, Mr. Hiroshi Kiyonari, Ms. Rika Nakayama, Ms. Ayako Nagao, and Ms. Kuniko Kitajima for their assistance. This work was supported in part by grants-in-aid for Scientific Research on Priority Areas and Young Scientists (B) from the Ministry of Education, Culture, Sports Science and Technology, Japan.

Received: September 24, 2004
Revised: April 28, 2005
Accepted: September 22, 2005
Published: October 31, 2005

References

Batten, B.E., and Haar, J.L. (1979). Fine structural differentiation of germ layers in the mouse at the time of mesoderm formation. Anat. Rec. *194*, 125–141.

Beddington, R.S., and Robertson, E.J. (1999). Axis development and early asymmetry in mammals. Cell *96*, 195–209.

Belo, J.A., Bouwmeester, T., Leyns, L., Kertesz, N., Gallo, M., Follettie, M., and De Robertis, E.M. (1997). *Cerberus-like* is a secreted factor with neutralizing activity expressed in the anterior primitive endoderm of the mouse gastrula. Mech. Dev. *68*, 45–57.

Brault, V., Moore, R., Kutsch, S., Ishibashi, M., Rowitch, D.H., McMahon, A.P., Sommer, L., Boussadia, O., and Kemler, R. (2001). Inactivation of the β-catenin gene by Wnt1-Cre-mediated deletion results in dramatic brain malformation and failure of craniofacial development. Development *128*, 1253–1264.

Brennan, J., Lu, C.C., Norris, D.P., Rodriguez, T.A., Beddington, R.S., and Robertson, E.J. (2001). Nodal signalling in the epiblast patterns the early mouse embryo. Nature *411*, 965–969.

Ciruna, B., and Rossant, J. (2001). FGF signaling regulates mesoderm cell fate specification and morphogenetic movement at the primitive streak. Dev. Cell *1*, 37–49.

Glinka, A., Wu, W., Delius, H., Monaghan, A.P., Blumenstock, C., and Niehrs, C. (1998). Dickkopf-1 is a member of a new family of secreted proteins and functions in head induction. Nature *391*, 357–362.

Imai, K., Takada, N., Satoh, N., and Satou, Y. (2000). (β)-catenin mediates the specification of endoderm cells in ascidian embryos. Development *127*, 3009–3020.

Kimura, C., Yoshinaga, K., Tian, E., Suzuki, M., Aizawa, S., and Matsuo, I. (2000). Visceral endoderm mediates forebrain development by suppressing posteriorizing signals. Dev. Biol. *225*, 304–321.

Kimura, C., Shen, M.M., Takeda, N., Aizawa, S., and Matsuo, I. (2001). Complementary functions of Otx2 and Cripto in initial patterning of mouse epiblast. Dev. Biol. *235*, 12–32.

Lewandoski, M., Meyers, E.N., and Martin, G.R. (1997). Analysis of Fgf8 gene function in vertebrate development. Cold Spring Harb. Symp. Quant. Biol. *62*, 159–168.

Logan, C.Y., and Nusse, R. (2004). The Wnt signaling pathway in development and disease. Annu. Rev. Cell Dev. Biol. *20*, 781–810.

Logan, C.Y., Miller, J.R., Ferkowicz, M.J., and McClay, D.R. (1999). Nuclear β-catenin is required to specify vegetal cell fates in the sea urchin embryo. Development *126*, 345–357.

Mao, B., Wu, W., Davidson, G., Marhold, J., Li, M., Mechler, B.M., Delius, H., Hoppe, D., Stannek, P., Walter, C., et al. (2002). Kremen proteins are Dickkopf receptors that regulate Wnt/β-catenin signalling. Nature *417*, 664–667.

Matsuo, I., Kuratani, S., Kimura, C., Takeda, N., and Aizawa, S. (1995). Mouse Otx2 functions in the formation and patterning of rostral head. Genes Dev. *9*, 2646–2658.

Mesnard, D., Filipe, M., Belo, J.A., and Zernicka-Goetz, M. (2004). The anterior-posterior axis emerges respecting the morphology of the mouse embryo that changes and aligns with the uterus before gastrulation. Curr. Biol. *14*, 184–196.

Mukhopadhyay, M., Shtrom, S., Rodriguez-Esteban, C., Chen, L., Tsukui, T., Gomer, L., Dorward, D.W., Glinka, A., Grinberg, A., Huang, S.P., et al. (2001). Dickkopf1 is required for embryonic head induction and limb morphogenesis in the mouse. Dev. Cell *1*, 423–434.

Niwa, H., Yamamura, K., and Miyazaki, J. (1991). Efficient selection for high-expression transfectants with a novel eukaryotic vector. Gene *108*, 193–199.

Perea-Gomez, A., Lawson, K.A., Rhinn, M., Zakin, L., Brulet, P., Mazan, S., and Ang, S.L. (2001). Otx2 is required for visceral endoderm movement and for the restriction of posterior signals in the epiblast of the mouse embryo. Development *128*, 753–765.

Popperl, H., Schmidt, C., Wilson, V., Hume, C.R., Dodd, J., Krumlauf, R., and Beddington, R.S. (1997). Misexpression of Cwnt8C in the mouse induces an ectopic embryonic axis and causes a truncation of the anterior neuroectoderm. Development *124*, 2997–3005.

Schneider, S., Steinbeisser, H., Warga, R.M., and Hausen, P. (1996). β-catenin translocation into nuclei demarcates the dorsalizing centers in frog and fish embryos. Mech. Dev. *57*, 191–198.

Srinivas, S., Rodriguez, T., Clements, M., Smith, J.C., and Beddington, R.S. (2004). Active cell migration drives the unilateral movements of the anterior visceral endoderm. Development *131*, 1157–1164.

Staal, F.J.T., van Noort, M., Strous, G.S., and Clevers, H.C. (2002). Wnt signals are transmitted through N-terminally dephosphorylated β-catenin. EMBO Rep. *3*, 63–68.

Stern, C.D. (2001). Initial patterning of the central nervous system: how many organizers? Nat. Rev. Neurosci. *2*, 92–98.

Thomas, P.Q., Brown, A., and Beddington, R.S. (1998). Hex: a homeobox gene revealing peri-implantation asymmetry in the mouse embryo and an early transient marker of endothelial cell precursors. Development *125*, 85–94.

Wikramanayake, A.H., Hong, M., Lee, P.N., Pang, K., Byrum, C.A., Bince, J.M., Xu, R., and Martindale, M.Q. (2003). An ancient role for nuclear beta-catenin in the evolution of axial polarity and germ layer segregation. Nature *426*, 446–450.

Wilkinson, D.G. (1998). In Situ Hybridization: A Practical Approach, Second Edition (Oxford/New York: Oxford University Press).

Yamamoto, M., Saijoh, Y., Perea-Gomez, A., Shawlot, W., Behringer, R.R., Ang, S.L., Hamada, H., and Meno, C. (2004). Nodal antagonists regulate formation of the anteroposterior axis of the mouse embryo. Nature *428*, 387–392.

Zakin, L., Reversade, B., Virlon, B., Rusniok, C., Glaser, P., Elalouf, J.M., and Brulet, P. (2000). Gene expression profiles in normal and Otx2$^{-/-}$ early gastrulating mouse embryos. Proc. Natl. Acad. Sci. USA *97*, 14388–14393.